Available online at www.sciencedirect.com

SciVerse ScienceDirect

Ceramics International 39 (2013) 3613–3620

CERAMICS INTERNATIONAL

www.elsevier.com/locate/ceramint

The influence of microstructure and phase composition of glass ceramics in the VO_2–V_2O_5–P_2O_5–Cu_2O–SnO_2 system on the electrical properties related to the metal–semiconductor phase transition

V.R. Kolbunov[a,*], A.I. Ivon[a], Y.A. Kunitskiy[b], I.M. Chernenko[c]

[a]*Department of Physics, Electronics and Computer Systems, Dnipropetrovsk National University,49010 Dnipropetrovsk, Ukraine*
[b]*Department of Physics, Taras Shevchenko National University of Kyiv, 01608 Kyiv, Ukraine*
[c]*Ukrainian State University of Chemical Technology, 49005 Dnipropetrovsk, Ukraine*

Received 10 August 2012; received in revised form 10 October 2012; accepted 11 October 2012
Available online 23 October 2012

Abstract

Phase composition, microstructure and electrical conductivity of glass ceramics in the VO_2–V_2O_5–P_2O_5–SnO_2 and VO_2–V_2O_5–P_2O_5–Cu_2O–SnO_2 systems have been studied. Only crystalline phases VO_2, SnO_2 and vanadium phosphate glass of the V_2O_5–P_2O_5 system have been found in glass ceramic compositions in the VO_2–V_2O_5–P_2O_5–SnO_2 system. Besides the above-mentioned phases, probably the X-ray lines of V_3O_5, V_4O_7, V_5O_9, V_6O_{11}, V_7O_{13}, V_4O_9, V_6O_{13}, V_2O_5, SnO_2, SnO, Sn_2O_3, Sn_3O_4 and CuO phases are observed in the X-ray spectra of glass ceramics in the VO_2–V_2O_5–P_2O_5–Cu_2O–SnO_2 system. According to SEM/EDS data, these phases were observed as submicrometer fine-crystalline inclusions in glass on the surface of VO_2 crystallites and between them. The formation of these phases was caused by the redox processes in the liquid phase during glass ceramics synthesis. The important role of tin oxides possessing high electrical conductivity and vanadium oxides exhibiting a low temperature of metal–semiconductor phase transition in the stabilization of glass ceramics electrical properties related to the phase transition in VO_2 has been established.

Keywords: B. Microstructure; C. Electrical conductivity; VO_2-based glass ceramics; X-ray analysis

1. Introduction

Vanadium dioxide (VO_2) undergoes the metal–semiconductor phase transition (MSPT) at the temperature of 341 K [1]. Such phase transition is accompanied by a jump of electrical conductivity and optical parameters [2–4]. This phenomenon attracts considerable scientific interest from the standpoint of its general theoretical description and practical application. In recent years, nanocrystalline vanadium dioxide [5,6] and VO_2 based ceramic materials [7] attracted the attention of researchers. The phase transition in VO_2 nanocrystals takes place in less than a few tens of femtoseconds [8], which makes it possible to use VO_2 for manufacturing high-speed optical modulators [9] and infrared detectors [10]. Ceramic materials based on VO_2 and vanadium phosphate glasses (VPG) of the V_2O_5–P_2O_5 system have attracted a significant interest because they can be used in the electronic components applicative at high electric currents [11]. This allows creating such components as critical thermistors which combine the characteristics of negative temperature coefficient thermistors and thermal relays. These thermistors can be used for inrush current limiting and for CPU protection from overheating.

The low stability of electric parameters during the thermocycling through the MSPT temperature is an essential disadvantage of VO_2-based volumetric polycrystalline and ceramic materials [12]. It is caused by the modification of the vanadium dioxide crystal cell during the phase transition [13]. This modification results in considerable mechanical stresses in the material. These

*Corresponding author.
E-mail address: sv@sobor.net (V.R. Kolbunov).

0272-8842/$ - see front matter © 2012 Elsevier Ltd and Techna Group S.r.l. All rights reserved.
http://dx.doi.org/10.1016/j.ceramint.2012.10.189

stresses lead to the microcracking that result in the rupture of electrical connections between VO_2 crystallites. As this takes place, the material loses its electrical properties related to the metal–semiconductor phase transition.

The research has shown that the addition of copper and tin dioxide to glass ceramics of the VO_2–V_2O_5–P_2O_5 system essentially improves the stability of electric parameters [12]. The results obtained suggest that the problem of the electrical parameters stabilization in VO_2-based glass ceramic materials can be solved. The solution of this problem implies not only the search of new stable glass ceramic compositions, but also the revealing of causes which may lead to the stabilization of properties related to the metal–semiconductor phase transition in VO_2.

Glass ceramic materials in the VO_2–V_2O_5–P_2O_5–Cu_2O–SnO_2 system are promising for the solution of the stabilization problem. The aim of this work is to study the microstructure and phase composition of such materials and investigate their influence on the glass ceramic properties related to the metal–semiconductor phase transition in vanadium dioxide.

2. Experimental

The industrial oxides V_2O_5 ($\geq$ 98.5%, Ural chemical plant, Pishma, Russia), SnO_2 (99%, RedMedSplav, Yekaterinburg, Russia), Cu_2O ($\geq$ 98.5%, Ural Mining and Smelting Company, Pishma, Russia) and dihydrogen phosphate $NH_4H_2PO_4$ (98%, SCI Co., Chifang, China) were used as starting materials for glass ceramics producing. The vanadium dioxide powder with particle sizes of 5–10 μm and VO_2 weight content of no less than 98% was obtained by the method described in Ref. [14].

The fabrication method for (mol%) $80V_2O_5$–$20P_2O_5$ vanadium phosphate glass is described in Ref. [15]. Appropriate quantities of VO_2, glass, Cu_2O and SnO_2 were weighed according to the ceramics composition and mixed. After homogenization we pressed the mixture under the pressure of 10^6 Pa and placed the pressed samples into a silica tube, which next was evacuated up to a pressure of about 0.1 Pa and filled with argon. The tube was placed into a furnace heated up to 1220 ± 10 K. After warming during 15–20 min, the tube was extracted for cooling up to room temperature. By this method, various compositions of glass ceramics in the VO_2–V_2O_5–P_2O_5–Cu_2O–SnO_2 system with a general formula (wt%) $4OVO_2$–15VPG–αCu_2O–$(45-\alpha)SnO_2$ and α within the range of $0 \leq \alpha \leq 10$ were obtained.

X-ray analysis was carried out using CuKα radiation ($\lambda = 0.15418$ nm) by means of the DRON-3M diffractometer (Burevestnik Co., Russia). JCPDS files were used for the identification of crystalline phases. The glass ceramics microstructure investigation was conducted on the scanning electron microscope JCXA-733 (JOEL Co., Japan). This device was also used for the X-ray elemental microanalysis by means of the energy dispersive X-ray spectroscopy (EDS). In order to study the electrical conductivity temperature dependences, cylindrical ceramic specimens of 10 mm diameter and the thickness of 1–1.5 mm with electrodes of 5 mm diameter on the bases were used. In–Ga eutectic was used as an electrode material. The temperature dependences of the sample electrical resistances were recorded at the heating rate of no more than 1 K per minute. The resistance was measured with a relative error of $\pm 0.1\%$ using the MO-62 dc bridge. The absolute error of the temperature record did not exceed ± 0.25 K.

3. Results

Fig. 1 illustrates a diffraction pattern typical of glass ceramics in VO_2–V_2O_5– P_2O_5–SnO_2 system. Ceramic compositions of this system have only two crystalline phases: monoclinic VO_2 and tetragonal SnO_2. A halo at the low angles indicates that there is an amorphous phase, viz. vanadium phosphate glass of V_2O_5–P_2O_5 system.

The absence of new phases in glass ceramics of the VO_2–V_2O_5–P_2O_5–SnO_2 system indicates that the liquid phase into which the VPG transforms at the synthesis temperature of $\sim 1220 \pm 10$ K is chemically neutral to VO_2 and SnO_2 oxides. These oxides have a high melting point and they stay solid during the synthesis.

It is known that VPG of the (mol%) $80V_2O_5$–$20P_2O_5$ composition crystallizes during the thermal treatment and liberates V_2O_5 and $VOPO_4$ phases [16]. Therefore, the X-ray phase analysis of glass ceramics in the VO_2–V_2O_5–P_2O_5–SnO_2 system yielded the results which conform to the data obtained in Refs. [17,18]. According to Ref. [17], new phases do not form in the V_2O_5–SnO_2 system. The authors of Ref. [18] have found that solid VO_2 poorly dissolves in the melt of V_2O_5 (the solubility limit of VO_2 is $\sim$1% of the melt mass at 1220 K).

The data of X-ray phase analysis for the two glass ceramics compositions in the VO_2–V_2O_5–P_2O_5–Cu_2O–SnO_2 system are shown in Fig. 2. These data show that on introducing cuprous oxide Cu_2O into VO_2-V_2O_5-P_2O_5-SnO_2 system, the phase composition of a glass ceramic

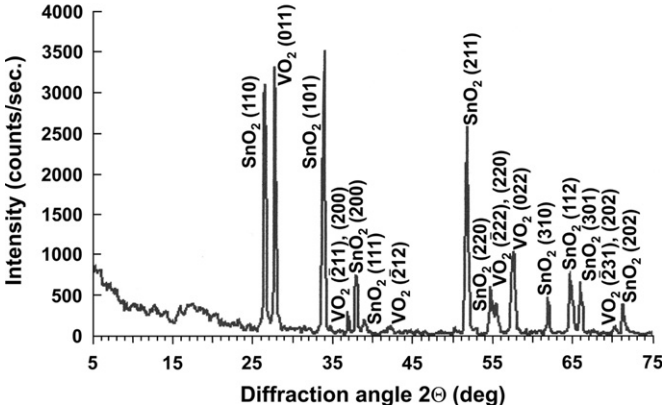

Fig. 1. X-ray diffraction pattern of (wt%) $45VO_2$–15VPG–$40SnO_2$ glass–ceramics.

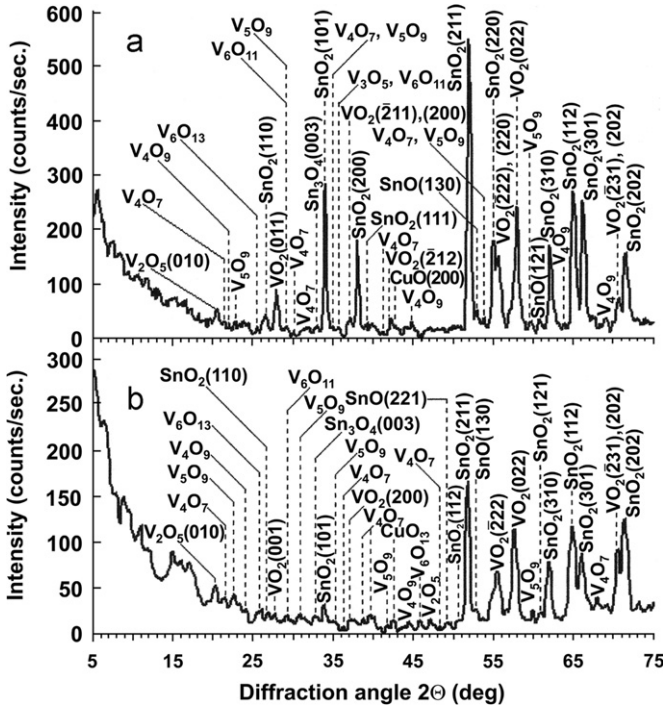

Fig. 2. The results of X-ray phase analysis for glass–ceramics of compositions (wt%): (a) $40VO_2$–15VPG–$39SnO_2$–$6Cu_2O$ and (b) $40VO_2$–15VPG–$37SnO_2$–$10Cu_2O$.

became compound. New lines were observed in the X-ray spectrum and the intensity of VO_2 and SnO_2 spectral lines decreased considerably. When the Cu_2O content was more than 8 wt%, the main spectral lines of VO_2 (011) and SnO_2 (110, 101) had a low intensity. The halo in the low-angle region indicates the presence of a glass phase.

The X-ray spectrums has the strongest change with the Cu_2O content growth in the region of the angles $2\theta < 50^\circ$, where the main X-ray lines of VO_2 and SnO_2 are localized. In this angle region many the faint lines are observed. According to JCPDS files some of these lines (Fig. 2) can be presumptively identified as the main lines of crystalline phases VO_2, V_2O_5, SnO_2, SnO, Sn_3O_4, CuO, Magneli phases V_nO_{2n-1} (V_3O_5, V_4O_7, V_5O_9, V_6O_{11}), and V_4O_9, V_6O_{13} phases. The dependable identification of these phases requires an additional investigation.

The diversity of phase compositions of glass ceramics in the VO_2–V_2O_5–P_2O_5–Cu_2O–SnO_2 system indicates that addition of Cu_2O caused redox reactions during the ceramics synthesis. Various lower vanadium and tin oxides were the products of these reactions. The emergence of CuO oxide testifies that Cu_2O is a reducing agent. A decrease in the intensity of VO_2 (011) X-ray line and the formation of an intermediate phase between VO_2 and V_2O_5 indicate that cuprous oxide interacts both with VO_2 and V_2O_5 in the liquid phase. The significant decrease in an intensity of basic SnO_2 X-ray lines after Cu_2O was introduced and the formation of SnO and Sn_3O_4 oxides show that SnO_2 undergoes reduction during the synthesis. The redox processes change the composition of glass, causing its fractional crystallization. This is confirmed by the appearance of the V_2O_5 main line (010) in the glass ceramics X-ray spectrum.

SEM images of the surface microstructure of different glass–ceramic compositions are shown in Fig. 3. glass ceramics of the VO_2–V_2O_5–P_2O_5–Cu_2O–SnO_2 system are heterogeneous materials. Their microstructure has such large-sized components as VO_2 and SnO_2 crystalline particles and pores. The size of VO_2 crystallites ranges between 3.5 μm and 25 μm. The surface of VO_2 crystallites is partly covered with a glass phase which has inclusions of fine crystallites of submicrometer sizes. Such crystallites can form aggregates consisting of rounded particles, or they can have a filamentary form with identical directivity within the aggregate. The proportion of filamentary crystallites grows with the increase of Cu_2O content. The large-sized VO_2 crystallites appear mostly as particles of an irregular shape, though VO_2 crystallites shaped as quadrangular prisms with the pyramidal bases also occur.

SnO_2 crystallites exist in the glass ceramics microstructure as octahedral particles with the size of 5 μm to 17 μm. SnO_2 crystallites 1 μm and less in size are localized in the glass phase as inclusions. These crystallites fill up the gaps between VO_2 and SnO_2 large-sized crystallites, and they are also situated on their surfaces. According to SEM/EDS data, the aggregates of rounded submicrometer crystallites are enriched by tin. Therefore, these aggregates may contain tin oxides.

A peculiarity of all the glass–ceramic compositions examined is their considerable porosity (Fig. 4a). The size of pores varies between 5 μm and 50 μm.

Typical maps that illustrate the distribution of elements over the scanned areas of ceramic materials in the VO_2–V_2O_5–P_2O_5–Cu_2O–SnO_2 system are shown in Fig. 4b–d. The data in Fig. 4b show that vanadium atoms are located in VO_2 crystallites and in the glass phase filling up the gaps between the crystallites. Fig. 4b shows that filamentary crystallites in the glass phase are enriched by vanadium. These crystallites can be Magneli phases V_nO_{2n-1} or phases that are intermediate between VO_2 and V_2O_5 with a general formula of V_nO_{2n+1}. Such phases were identified on the base of the above mentioned X-ray data.

According to the map in Fig. 4c, tin atoms are located in large-sized octahedral SnO_2 crystallites and in rounded crystallites of submicrometer sizes filling the gaps between the larger VO_2 crystallites or situated on the surface of these crystallites. Considering the X-ray data, we can assume that the aggregates of tin-enriched microcrystalline particles are a mixture of SnO_x tin oxides, where x has the values of 1, 4/3 and 2.

According to Fig. 4d, copper atoms are located in glass phase areas. The copper atoms concentration on the open surface of VO_2 crystallites is low. This suggests that during the ceramics synthesis, Cu_2O dissolves in the liquid phase which transforms into glass at the cooling stage. This conforms to the results of glass ceramics study in the VO_2–V_2O_5–P_2O_5–Cu system [14], where the dissolution of copper in the liquid phase during the ceramics synthesis was reported.

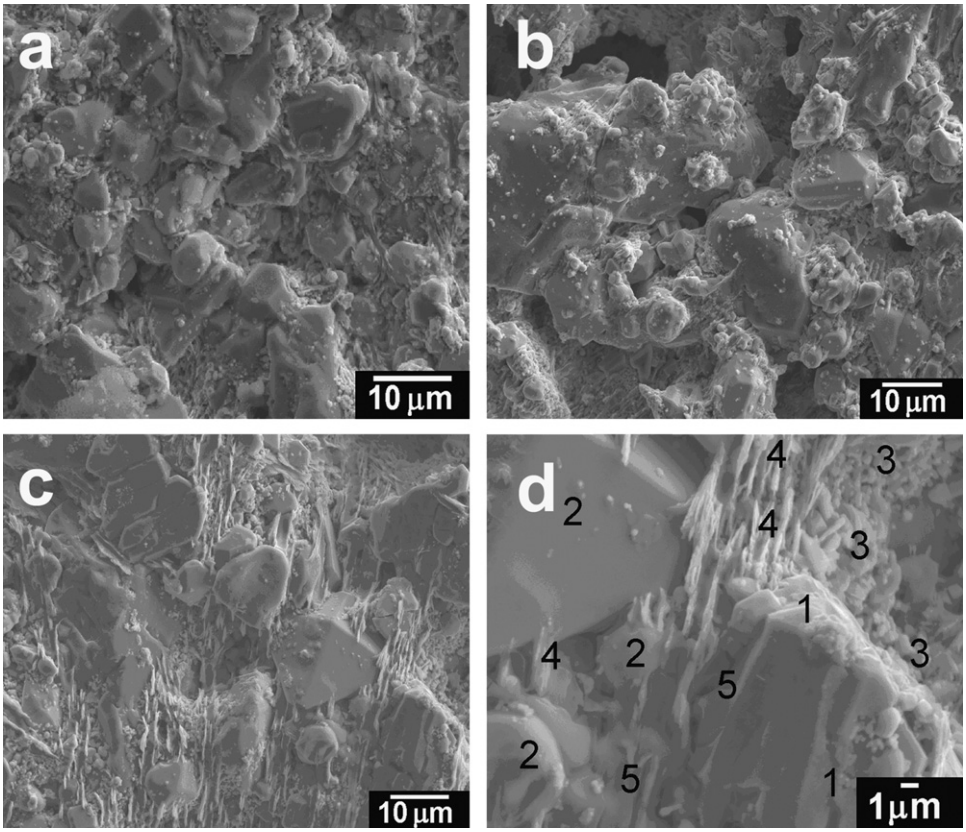

Fig. 3. SEM images of the surface for glass–ceramics of compositions: (a) $40VO_2$–$15B\Phi C$–$39SnO_2$–$6Cu_2O$; (b) $40VO_2$–$15B\Phi C$–$37SnO_2$–$8Cu_2O$ and (c), (d) $40VO_2$–$15B\Phi C$–$35SnO_2$–$10Cu_2O$. 1—VO_2 crystallites; 2—SnO_2 crystallites; 3— SnO_x submicrometer crystallites; 4—V_nO_{2n-1} and V_nO_{2n+1} filamentary crystallites and 5—glass phase.

The study of the copper distribution map revealed that the glass–ceramic microstructure has certain regions of ~1–2 μm in size exhibiting high concentrations of copper atoms. Probably, the crystallites of CuO phase were located in these regions. The presence of CuO in the investigated glass ceramic compositions was confirmed by X-ray data (Fig. 2).

A highly magnified SEM image of the surface area of glass ceramics having the composition (wt%) $40VO_2$–15VPG–$35SnO_2$–$10Cu_2O$ is shown in Fig. 3d. Fig. 3d illustrates the phases marked according to SEM/EDS and X-ray phase analysis data. As it can be seen in Fig. 3c and d, the filamentary crystals of V_nO_{2n-1} and V_nO_{2n+1} phases create the bridges between the large-sized VO_2 crystallites. Since many Magneli and V_6O_{13} phases are in the metallic state at room temperature [19,20], these bridges create low-resistance electrical couplings between VO_2 crystallites in the glass ceramics.

The temperature dependences of electrical conductivity σ in glass ceramic samples of various systems are shown in Fig. 5. Apparently, the addition of SnO_2 and Cu_2O sufficiently affects both the value and the behavior pattern of electrical conductivity during the temperature changes.

The glass ceramic samples of the same $85VO_2$–15VPG composition in the VO_2–V_2O_5–P_2O_5 system may exhibit different temperature dependences of σ, which are shown as curves 3 and 6 in Fig. 5. The temperature dependence of the electrical conductivity σ (T) may show the behavior typical of the metal–semiconductor phase transition in VO_2. This is characterized by a sharp increase of σ (a conductivity jump) observed in the vicinity of $T_t = 341$ K over more than two decades (Fig. 5, curve 3). Sometimes, σ (T) does not exhibit this type of behavior (Fig. 5, curve 6). In this case, a glass ceramic sample of the above composition will possess considerably lower electrical conductivity that will not increase but decrease in the vicinity of T_t.

SnO_2 added to the VO_2–V_2O_5–P_2O_5 system (VO_2–V_2O_5–P_2O_5–SnO_2 system) causes the temperature behavior of the glass ceramics conductivity, which is typical of a metal–semiconductor phase transition in VO_2. All ceramics samples of the VO_2–V_2O_5–P_2O_5–SnO_2 system that were investigated exhibited a σ jump by no less than two orders in the vicinity of $T_t = 341$ K (Fig. 5, curve 4).

This type of σ (T) behavior caused by the phase transition in VO_2 is exhibited by various glass ceramic compositions in the VO_2–V_2O_5–P_2O_5–Cu_2O–SnO_2 system (Fig. 5, curves 1, 2, and 5). The characteristic properties of glass ceramics in this system are an increase in σ and a certain shift of the conductivity jump to the low temperature region with increasing the Cu_2O content.

The effect of thermocycling through $T_t = 341$ K on the conductivity of various glass ceramic compositions is illustrated in Fig. 6.

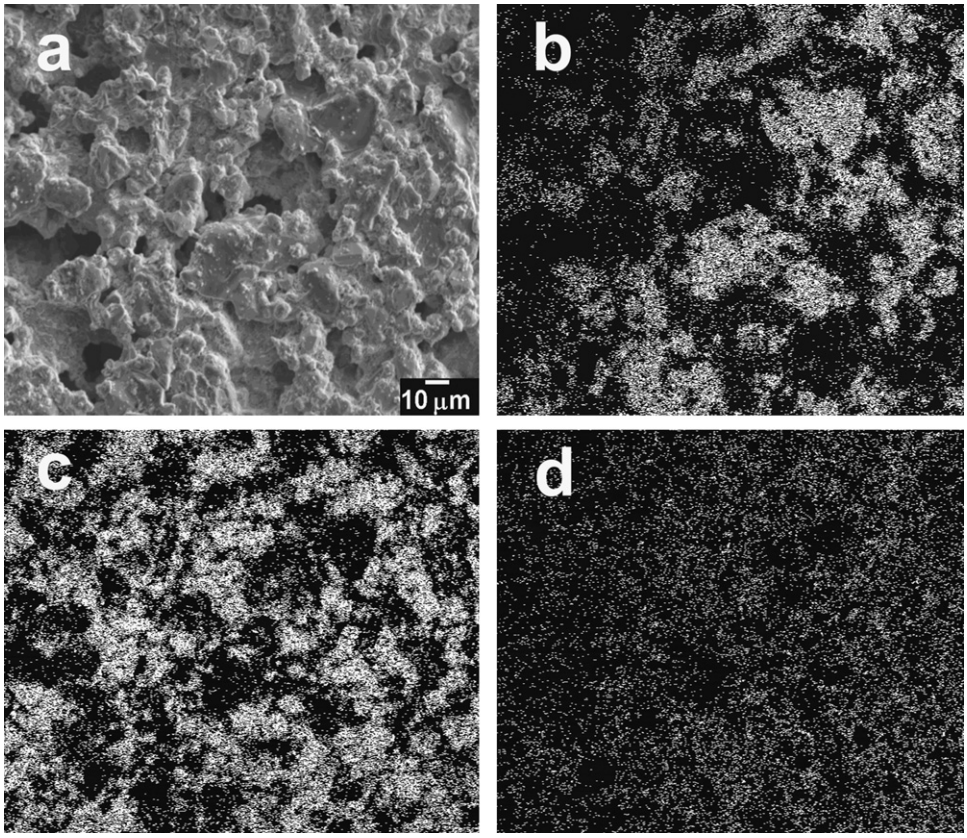

Fig. 4. (a) SEM micrograph of the surface for glass–ceramics $40VO_2$–$15B\Phi C$–$37SnO_2$–$8Cu_2O$ and maps the distribution of elements over the scanned area: (b) vanadium; (c) tin and (d) copper.

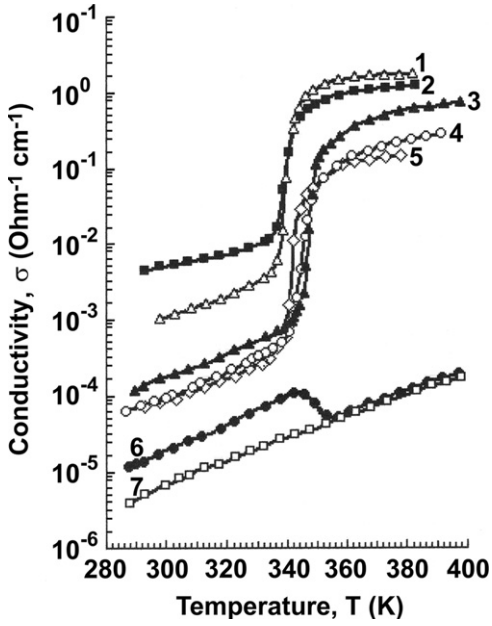

Fig. 5. Temperature dependences of specific conductivity in VPG (7) and glass–ceramics of compositions (wt%): (1) $40VO_2$–$15VPG$–$35SnO_2$–$10Cu_2O$; (2) $40VO_2$–$15VPG$–$37SnO_2$–$8Cu_2O$; (3, 6) $85VO_2$–$15VPG$; (4) $40VO_2$–$15VPG$–$45SnO_2$; (5) $40VO_2$–15 VPG–$39SnO_2$–$6Cu_2O$.

glass ceramics of $85VO_2$–$15VPG$ composition are very unstable during the thermocycling. Though there is no mechanical specimen destruction due to microcracking, the electrical resistance of the compositions increases more than thousand times, and the MSPT-related conductive jump in vanadium dioxide does not occur after about 20 thermal cycles. The doping with SnO_2 considerably improves the stability of electrical properties. glass ceramics of $65VO_2$–$15VPG$–$20SnO_2$ composition exhibit an increase in the electric resistance approximately by an order after 100 thermal cycles. However, it should be noticed that after 10–15 thermal cycles, the magnitude of the conductivity jump in the vicinity of temperature T_t starts dropping with further thermal cycles. Cu_2O doping results in the additional improvement of stability. Fig. 6 (curves 3, 4) shows that stabilization of the electric resistance is observed with the growing number of thermal cycles. The electric resistance increases not more than three times after 100 thermal cycles. The magnitude of the conductivity jump in the vicinity of T_t was constant during the thermocycling for all the glass ceramic compositions of VO_2–V_2O_5–P_2O_5–Cu_2O–SnO_2 system.

4. Discussion

On the base of the above data, a microstructure formation mechanism in the synthesis of glass ceramics in the VO_2–V_2O_5–P_2O_5–Cu_2O–SnO_2 system can be suggested. Vanadium phosphate glass (the softening temperature of ~530 K [21]) is in the liquid state of low viscosity at the

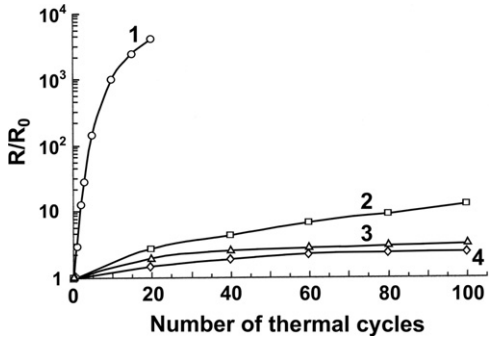

Fig. 6. The dependence of relative resistance change at 290 K on the number of thermal cycles through the MSPT temperature $T_t = 341$ K for glass–ceramics of compositions (wt%): (1) $85VO_2$–15VPG; (2) $65VO_2$–15VPG–$20SnO_2$; (3) $40VO_2$–15VPG–$39SnO_2$–$6Cu_2O$ and (4) $40VO_2$–15VPG–$37SnO_2$–$8Cu_2O$.

synthesis temperature of 1220 K. The other burden constituents are to be in the solid state, having a melting point above 1500 K. However, according to the SEM/EDS data, Cu_2O dissolves in the liquid phase. Furthermore, a partial dissolution of VO_2 solid particles is expected, since V_2O_5 is included as a component of liquid phase [18]. The solid particles of SnO_2 may also dissolve partially in the liquid phase, as in V_2O_5–SnO_2 system the nonvariant equilibrium with eutectic temperature of 898 K takes place [17]. The above-listed processes change the liquid phase composition.

If no Cu_2O is added, then no redox reactions occur during the ceramics synthesis. Therefore, the phase composition of glass ceramics in the VO_2–V_2O_5–P_2O_5–SnO_2 system (Fig. 1) does not differ from the burden phase composition used for its fabrication. The dissolution of VO_2 and SnO_2 solid particles continues until the liquid phase is saturated by these oxides. Because of this, the major part of VO_2 and SnO_2 oxides stay solid during the ceramics synthesis. The liquid phase as well as vanadium and tin dioxides dissolved in it promote a process of mass transfer causing the growth of VO_2 and SnO_2 crystallites during the ceramics synthesis. VO_2 and SnO_2 oxides dissolved in the liquid phase crystallize at the cooling stage as the solubility limit decreases. It is confirmed by the presence of fine-crystalline particles in the glass phase, which can be observed in SEM images of glass ceramics in the VO_2–V_2O_5–P_2O_5–SnO_2 system. On cooling, the liquid phase turns into the solid phase referred to as VPG. This glass holds ceramics crystallites together, which imparts high mechanical strength to the material.

The addition of Cu_2O to the burden composition results in redox processes between the components dissolved in the liquid phase. These processes can be described by the following reactions:

$$nVO_2 + Cu_2O \leftrightarrow V_nO_{2n-1} + 2CuO, \text{ where } n = 3, 4, 5, 6; \quad (1)$$

$$nV_2O_5 + (n-2)\ Cu_2O \leftrightarrow 2V_nO_{2n+1} + (2n-4)\ CuO, \text{ where } n = 4, 6; \quad (2)$$

$$SnO_2 + (2-x)\ Cu_2O \leftrightarrow SnO_x + (4-2x)\ CuO, \text{ where } x = 1, 4/3. \quad (3)$$

Reaction (1) leads to the crystallization of Magneli phases; reaction (2) results in the crystallization of vanadium oxides that are intermediate between VO_2 and V_2O_5 phases; reaction (3) explains the formation of lower tin oxides in the glass ceramic compositions of the VO_2–V_2O_5–P_2O_5–Cu_2O–SnO_2 system. Apparently, as these phases have a high melting point their crystallization can take place either at the stage of heating up to the maximum synthesis temperature of ~1220 K or at the stage of cooling down from this temperature level. Since the redox processes change the liquid phase composition, this leads to the fractional crystallization of vanadium phosphate glass at the cooling stage. This process explains the appearance of the line inherent for the crystalline V_2O_5 in the X-ray spectrum (Fig. 2). This line can also be associated with glass-forming properties of the CuO–P_2O_5 system [22]. So CuO oxide forming in the liquid phase as a result of reactions (1–3) can form some glass of the CuO–P_2O_5 system at the cooling stage. If this takes place, CuO can displace V_2O_5 out of the glass phase.

According to the above mentioned data, VO_2-based glass ceramics are a disordered heterogeneous system consisting of different crystalline phases, an amorphous phase and pores. Therefore, the electrical properties of such materials should be analyzed taking into account both the electrical conductivity of separate phases and the peculiarities of the glass ceramics microstructure. It is essential to understand the influence of glass ceramics microstructures and the conductivity of their separate components on electrical properties of these materials related to MSPT in vanadium dioxide. One of these properties which is of great value for practical applications is the conductivity jump in VO_2 in the vicinity of phase transition temperature $T_t = 341$ K.

The conductivity of a disordered heterogeneous system consisting of components that have different conductivities is described by the percolation theory [23,24]. According to this theory, any component of a heterogeneous system will contribute to its conductivity if percolation through this component occurs. It takes place if the volume fraction x of component exceeds the volume fraction x_c which conforms to the percolation threshold ($x_c \cong 0.25$ for cubic lattice in the bond percolation problem [24]). Hence, to impart the MSPT-related electrical properties to VO_2-based ceramics, it is necessary to provide percolation through VO_2 crystallites. Such percolation should take place when the volume fraction of VO_2 in ceramics x_v exceeds the value $x_c \cong 0.25$. The volume fraction x_v can be estimated from the VO_2 weight content C_v as $x_v = C_v d/d_v$, where d is the ceramics specific weight and $d_v \cong 4.4$ g/cm^3 is the specific weight of VO_2. The specific weight for ceramics of the composition $85VO_2$–15VPG is 2.9 g/cm^3. Therefore the volume fraction of VO_2 is $x_v = 0.56$ in such ceramics. The values of d are in the range (3.7–3.9) g/cm^3 for ceramics of composition $4OVO_2$–15VPG–αCu_2O–(45 – α)SnO_2 ($0 \le \alpha \le 10$) and the value of x_v should be in the range 0.34–0.35 without regard for the interaction between

VO_2 and Cu_2O during the ceramics synthesis. These values of the VO_2 volume fraction exceed the percolation threshold $x_c \cong 0.25$ and so it is necessary to expect the percolation through VO_2 crystallites. However as was mentioned above, sometimes the $85VO_2$–15VPG ceramics has a temperature dependence of conductivity is not typical for the phase transition in VO_2 (Fig. 5, curve 6). It testifies the absence of percolation through VO_2 crystallites, although x_v is $\sim$0.56 in this ceramics.

Such feature can be explained if taken into account the microstructure data. These data have shown [12,14] that vanadium phosphate glass in ceramics covers the surface of the large-sized VO_2 crystallites and forms the interlayers between them. The specific conductivity of VO_2 is near $10^{-1}\,\Omega^{-1}\,cm^{-1}$ at $\sim$290 K [1,4]. The specific conductivity of VPG is by 4–5 orders lower than the conductivity of VO_2 in semiconductor phase (Fig. 5, curve 7). The pores also exhibit low conductivity. Therefore, VPG interlayers and pores electrically isolate VO_2 crystallites from one another and make the major contribution to the glass ceramics conductivity. It explains why the percolation through VO_2 crystallites can be absent even if the VO_2 volume fraction exceeds the percolation threshold $x_c \cong 0.25$ (Fig. 5, curve 6). The percolation through the vanadium dioxide takes place in glass ceramics of the VO_2–V_2O_5–P_2O_5 system on condition that VO_2 crystallites have the sufficiently large number of direct electric contacts with each other. Such contacts are formed as a result of VO_2 crystallites coalescence during the synthesis, and at the cooling stage, due to the crystallization of VO_2 dissolved in a liquid phase. During crystallization the fine-crystalline VO_2 forms in the glass interlayers between the large-sized VO_2 crystallites. If the percolation through the fine-crystalline VO_2 localized in glass interlayers takes place, the additional electric contacts between the large-sized VO_2 crystallites are formed.

A sufficient number of the contacts will give rise to the percolation in VO_2 phase. In this case, an abrupt increase of σ is observed in the temperature dependence of glass ceramics conductivity in the vicinity of phase transition temperature $T_t = 341$ K (Fig. 5, curve 3). Otherwise, the VPG interlayers between large-scale VO_2 crystallites will make the major contribution to the ceramics conductivity. In this case, the conductivity may sharply decrease in the vicinity of temperature T_t (Fig. 5, curve 6). This is caused by mechanical stresses in the glass ceramics during the phase transition in VO_2 crystallites. These stresses result in microcracking, which causes a decrease in the effective specific conductivity of ceramics.

X-ray and SEM/EDS data indicate that the microstructure of the VO_2–V_2O_5–P_2O_5–SnO_2 system glass ceramics includes the following components: VO_2 crystallites, SnO_2 crystallites, vanadium-phosphate glass, and pores. The SEM data show that the inclusions of SnO_2 fine crystallites are located within the glass interlayers separating the VO_2 crystallites. Since SnO_2 has a high electrical conductivity of $\sim 80\,\Omega^{-1}\,cm^{-1}$ [25], its inclusions in glass create additional contacts between VO_2 crystallites in glass ceramics. SnO_2 fine crystallite inclusions in VPG interlayers actually perform the functions of electrical couplings between VO_2 crystallites. In comparison with the VO_2–V_2O_5–P_2O_5 system glass ceramics, these couplings additionally promote percolation through VO_2 crystallites. Therefore, the σ jump related to the phase transition in VO_2 was inevitably observed on the conductivity temperature dependence curve in every sample of glass ceramics in the VO_2–V_2O_5–P_2O_5–SnO_2 system (Fig. 5, curve 4). A more developed network of electrical couplings, which facilitates percolation through VO_2 crystallites, explains a more stable behavior of conductivity shown by the VO_2–V_2O_5–P_2O_5–SnO_2 system glass ceramics during the thermocycling (Fig. 6, curve 2). Many more thermal cycles are needed to destroy this network by microcracks forming during the MSPT in VO_2 crystallites.

The filamentous crystallites of Magneli phases and V_6O_{13}, additionally promote percolation through the VO_2 crystallites in the VO_2–V_2O_5–P_2O_5–SnO_2–Cu_2O system glass ceramics, as they are in the conducting metallic state over the temperature range under study. The SEM data show that these filamentous crystallites form bridges between the large-sized VO_2 crystallites. Hence, unlike glass ceramics in the VO_2–V_2O_5–P_2O_5 or VO_2–V_2O_5–P_2O_5–SnO_2 systems, the VO_2–V_2O_5–P_2O_5–SnO_2–Cu_2O system glass ceramics has a higher developed network of electrical couplings, which facilitates percolation through the VO_2 crystallites. This explains a better stability of glass ceramics conductivity in the VO_2–V_2O_5–P_2O_5–SnO_2–Cu_2O system (Fig. 6, curves 3, 4) and its better electrical properties related to the phase transition in VO_2.

5. Conclusion

According to the data of X-ray phase analysis, ceramic materials of VO_2–V_2O_5–P_2O_5–SnO_2 system contain the crystalline phases VO_2, SnO_2 and the amorphous phase, viz. vanadium phosphate glass. Therefore, a conclusion can be drawn that there is no interaction between the burden constituents during the synthesis of glass ceramics in this system.

Besides VO_2 and SnO_2 phases, the X-ray spectra of glass ceramics in the VO_2–V_2O_5–P_2O_5–SnO_2–Cu_2O system contain the lines which probably are the main lines of Magneli phases V_nO_{2n-1}, SnO_2, SnO, Sn_2O_3, V_2O_5, CuO oxides, and oxides having the V_nO_{2n+1} composition. This testifies that redox reactions occur and change the glass ceramics phase composition during the synthesis. The redox reactions occur in the liquid phase which contains V_2O_5 and the dissolved VO_2, SnO_2, Cu_2O oxides. Cuprous oxide acts as a reducing agent. It oxidizes to CuO in the reduction of V_2O_5, VO_2, SnO_2 oxides.

The SEM/EDS data show that the microstructure of glass ceramics in the VO_2–V_2O_5–P_2O_5–Cu_2O–SnO_2 system has the following components: VO_2 crystallites 3.5–25 μm in size, octahedral SnO_2 crystallites 5–17 μm in size,

submicrometer crystallites of tin oxide SnO_x ($x=1$, 4/3, 2), crystallites of the vanadium oxides V_3O_5, V_4O_7, V_5O_9, V_6O_{11}, V_4O_9, V_6O_{13} dispersed in glass, and pores. VPG together with crystallites of different phases dispersed in it covers the surfaces of VO_2 crystallites and forms the interlayers between them.

The fine crystallites of tin oxides and the Magneli phases are dispersed in the glass filling the gaps between VO_2 crystallites. They create a well-developed network of electrical couplings that provide the percolation through VO_2 crystallites. Thus, glass ceramics in the VO_2–V_2O_5–P_2O_5–Cu_2O–SnO_2 system attain electrical properties related to the metal–semiconductor phase transition in VO_2 and exhibit a better stability during the thermocycling through the phase transition temperature.

References

[1] F. Morin, Oxides which show a metal-to-insulator transition at the Neel temperature, Physical Review Letters 3 (1959) 34–36.

[2] L.A. Ladd, W. Paul, Optical and transport properties of high quality crystals of V_2O_4 near the metallic transition temperature, Solid State Communications 7 (1969) 425–428.

[3] D.H. Kim, H.S. Kwok, Pulsed laser deposition of VO_2 thin films, Applied Physics Letters 65 (1994) 3188–3190.

[4] V. Melnik, I. Khatsevych, V. Kladko, A. Kuchuk, V. Nikirin, B. Romanyuk, Low-temperature method for thermochromic high order VO_2 phase formation, Materials Letters 68 (2012) 215–217.

[5] F. Guinneton, J.-C. Valmalette, J.-R. Gavarri, Nanocrystalline vanadium dioxide: synthesis and mid-infrared properties, Optical Materials 15 (2000) 111–114.

[6] W.W. Li, J.J. Zhu, X.F. Xu, K. Jiang, Z.G. Hu, M. Zhu, J.H. Chu, Ultraviolet–infrared dielectric functions and electronic band structures of monoclinic VO_2 nanocrystalline film: temperature-dependent spectral transmittance, Journal of Applied Physics 110 (2011) 013504.

[7] Mengna Luo, Liuya Wei, Qun Fu, Deming Lei, Chenmou Zheng, The effect of stoichiometry of VO_2 nano-grain ceramics on their thermal and electrical properties, Materials Chemistry and Physics 104 (2007) 258–260.

[8] A. Cavalleri, Th. Dekorsy, H.H.W. Chong, J.C. Kieffer, R.W. Schoenlein, Evidence for a structurally-driven insulator-to-metal transition in VO_2: a view from the ultrafast timescale, Physical Review B 70 (2004) 161102 (R).

[9] M. Soltani, M. Chaker, E. Haddad, R. Kruzelecky, J. Margot, Micro-optical switch device based on semiconductor-to-metallic phase transition characteristics of W-doped VO_2 smart coatings, Journal of Vacuum Science and Technology 25 (2007) 971–975.

[10] Sihai Chen, Hong Ma, Sihua Xiang, Xinjian Yi, Fabrication and performance of microbolometer arrays based on nanostructured vanadium oxide thin films, Smart Materials and Structures 16 (2007) 696–700.

[11] A.I. Ivon, V.R. Kolbunov, I.M. Chernenko, Voltage–current characteristics of vanadium dioxide based ceramics, Journal of the European Ceramic Society 23 (2003) 2113–2118.

[12] A.I. Ivon, V.R. Kolbunov, I.M. Chernenko, Conductivity stabilization by metal and oxide additives in ceramics on the basis of VO_2 and glass V_2O_5–P_2O_5, Journal of Non-Crystalline Solids 351 (2005) 3649–3654.

[13] T. Kawakubo, T. Nakagawa, Phase transition in VO_2, Journal of Physical Society of Japan 19 (1964) 517–519.

[14] A.I. Ivon, I.M. Chernenko, V.R. Kolbunov, Phase composition, microstructure and conductivity of $(85-\alpha)VO_2$–15(vanadium-phosphate-glass)–αCu glass ceramics, Journal of Non-Crystalline Solids 353 (2007) 1521–1528.

[15] A.I. Ivon, V.R. Kolbunov, I.M. Chernenko, Stability of electrical properties of vanadium dioxide based ceramics, Journal of the European Ceramic Society 19 (1999) 1883–1888.

[16] A.I. Ivon, E.G. Ivon, I.M. Chernenko, Synthesis and crystallization process of glasses in the V_2O_5–P_2O_5 system, Glass Physics and Chemistry 9 (1983) 284–286.

[17] Y. Ivanova, V. Vassilev, S. Stefanova, M. Staneheva, Phase equilibrium in the SnO_2–V_2O_5 system, Journal of Materials Science Letters 12 (1993) 455–456.

[18] A.I. Ivon, I.M. Chernenko, A.P. Kudzina, Dissolution kinetics of vanadium dioxide crystals in a melt of vanadium oxide (V), Russian Journal of Physical Chemistry 62 (1988) 611–616.

[19] E.G. Goryachev, S.G. Ovchinnikov, Electrical and magnetic properties of Magneli phases V_nO_{2n-1}, Soviet physics, Solid state 20 (1978) 2201–2209.

[20] R. Eguchi, T. Yokoya, T. Kiss, Y. Ueda, S. Shin, Angle-resolved photoemission study of the mixed valence oxide V_6O_{13}: quasi-one-dimensional electronic structure and its change across the metal–insulator transition, Physical Review B 65 (2002) 205124.

[21] Biprodas Dutta, Niveen A. Fahmy, Ian L. Pegg, Effect of mixed transition-metal ions in glasses. I. The P_2O_5–V_2O_5–Fe_2O_3 system, Journal of Non-Crystalline Solids 351 (2005) 1958–1966.

[22] L. Murawski, C.H. Chung, J.D. Mackenzie, Electrical properties of semiconducting oxide glasses, Journal of Non-Crystalline Solids 32 (1979) 91–104.

[23] S. Kirkpatrick, Percolation and conduction, Reviews of Modern Physics 45 (1973) 574–588.

[24] B.I. Shklovskii, A.L. Efros, Electronic Properties of Doped Semiconductors, Springer-Verlag, Berlin Heidelberg, NewYork, Tokyo, 1984.

[25] M.-M. Bagheri-Mohagheghi, N. Shahtahmasebi, M.R. Alinejad, A. Youssefi, M. Shokooh-Saremi, Fe-doped SnO_2 transparent semi-conducting thin films deposited by spray pyrolysis technique: thermoelectric and p-type conductivity properties, Solid State Sciences 11 (2009) 233–239.